RESEARCH ARTICLE | SEPTEMBER 12 2023

The rheology of saltwater taffy 📵

San To Chan (陳新淘) ✉ 📵 ; Simon J. Haward 📵 ; Eliot Fried 📵 ; Gareth H. McKinley 📵
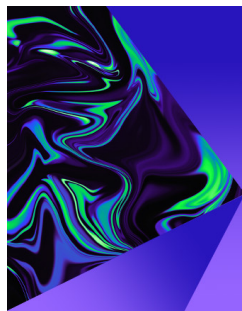
Check for updates

View Online   Export Citation   CrossMark

The rheology of saltwater taffy Ⓕ

View Online　　Export Citation　　CrossMark

San To Chan (陳新淘),[1,a)] ⓘ Simon J. Haward,[2] ⓘ Eliot Fried,[1] ⓘ and Gareth H. McKinley[3] ⓘ

AFFILIATIONS

[1]Mechanics and Materials Unit, Okinawa Institute of Science and Technology Graduate University, Onna, Okinawa 904-0495, Japan
[2]Micro/Bio/Nanofluidics Unit, Okinawa Institute of Science and Technology Graduate University, Onna, Okinawa 904-0495, Japan
[3]Department of Mechanical Engineering, Massachusetts Institute of Technology, Cambridge, Massachusetts 02139, USA

Note: This paper is part of the special topic, Special Issue on Food Physics.
[a)]Author to whom correspondence should be addressed: san.chan@oist.jp

ABSTRACT

Saltwater taffy, an American confection consisting of the main ingredients sugar, corn syrup, water, and oil, is known for its chewy texture and diverse flavors. We use a small amplitude oscillatory shear test to probe the linear viscoelastic properties of commercial taffy. At low frequencies, self-similar relaxation behavior characteristic of a critical gel is observed. The storage and loss moduli are power-law functions, with the same exponent, of the frequency. Such self-similarity arises from the distribution of air bubbles and oil droplets in the taffy, where air is incorporated and oil is emulsified through an iterative folding process known as "taffy-pulling." Taffy obeys the time–temperature superposition principle. Horizontally shifting the dynamic moduli obtained at different temperatures yields a master curve at a chosen reference temperature. As a sufficiently high frequency is exceeded, taffy transitions from a critical gel-like state to an elastic solid-like state. The master curve can be described by the fractional Maxwell gel (FMG) model with three parameters: a plateau modulus, a characteristic relaxation time, and a power-law exponent. The master curves for taffy of different flavors can all be described by the FMG model with the same exponent, indicating that minor ingredients like flavorings and colorings do not significantly affect the rheology of taffy. Scaling the master curves with the plateau modulus and relaxation time results in their collapse onto a supermaster curve, hinting at a more fundamental time–temperature–taffy superposition principle. Guided by this principle, we hand-pull lab-made model taffies successfully reproducing the rheology of commercial taffy.

I. INTRODUCTION

Saltwater taffy, the well-known American confection, has been a popular gift among locals and tourists for generations [see Fig. 1(a)]. Despite its name, saltwater taffy does not contain seawater. Instead, the name is believed to have originated from a humorous incident involving a candy store owner and a young child. In popular lore, the name is attributed to a candy store owner named David Bradley, whose shop in Atlantic City was flooded during a major storm in the late 1800s, soaking his entire stock of taffy in seawater. When a little girl came into the shop asking for taffy, Bradley jokingly offered her "saltwater taffy." The name then spread and became ubiquitous.[1]

The production of (saltwater) taffy typically involves boiling a mixture of sugar, corn syrup, water, and oil to the hard-ball or soft-crack stage, corresponding to the temperature range of 121–130 °C or 132–143 °C, respectively.[2] The cooked mixture is then poured onto a surface for cooling. Once the mixture has cooled to a temperature amenable to handling, it is stretched and folded repeatedly in a process known as "taffy-pulling."[3,4] This process aerates the candy and emulsifies the oil it contains, making it opaque and lightweight. Figure 1(b) shows the three-dimensional microstructure of a grape-flavored piece of taffy reconstructed by x-ray micro-computed tomography. Inclusions can be seen inside the candy, signifying aeration and emulsification. Traditionally, taffy pulling is performed by hand (Fig. 2), often during social gatherings and parties. In candy factories, the process is performed by taffy pullers, which are mechanical devices specialized in repeatedly stretching and folding highly viscous materials.[5–7] A representative toy taffy puller[8] is shown in Fig. 3(a). The puller consists of two rotatable arms and a fixed hook. As the arms move away from the hook, they catch and stretch the taffy [Figs. 3(b)–3(d)]. As they return, the taffy folds back onto itself [Figs. 3(e)–3(h)]. The process repeats as the arms continue to rotate. By inspecting Figs. 2 and 3, it is immediately evident that the taffy surface is much more irregular when a taffy puller is used. The history of stretching and folding imparted by the taffy puller more efficiently folds air into the candy.
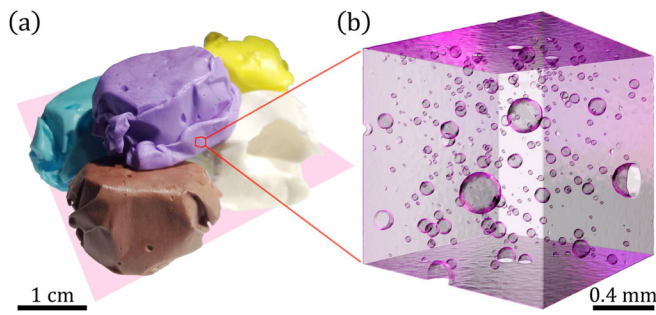
FIG. 1. (a) Saltwater taffy of various flavors and (b) a three-dimensional model reconstructed by x-ray micro-computed tomography showing polydisperse distributions of air bubbles and oil droplets in the grape-flavored variety.

In this article, we present a comprehensive study of the linear viscoelastic properties of saltwater taffy. We demonstrate that taffy is thermorheologically simple over the temperature window relevant to taffy processing. Taffy obeys the time–temperature superposition principle, an empirical law broadly followed by amorphous polymeric materials, which states that altering the temperature has an effect on the rheological behavior equivalent to that induced by changing the timescale of the applied deformation.[9] This characteristic allows us to construct rheological master curves that describe the linear viscoelastic response of taffy with various flavors under different deformation timescales at a chosen reference temperature. As the characteristic timescale of the deformation process decreases, the taffy transitions from a dissipative, liquid-like state at long timescales to an increasingly elastic, solid-like state at shorter timescales.[10] The master curve can be interpreted within the framework of fractional viscoelasticity using the
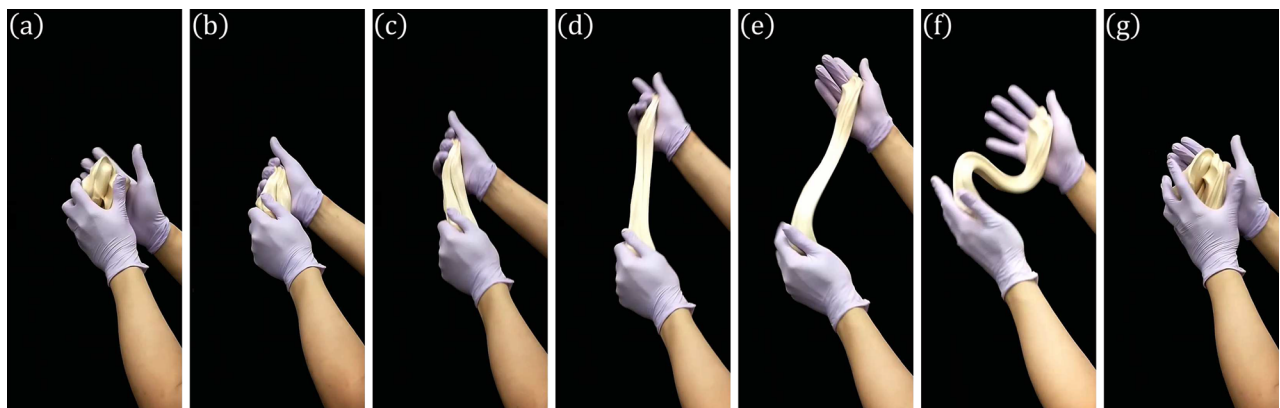
FIG. 2. Taffy pulling by hand. The taffy is repeatedly stretched and folded back onto itself until it becomes sufficiently aerated. The time interval separating successive images is ~ 0.1 s.
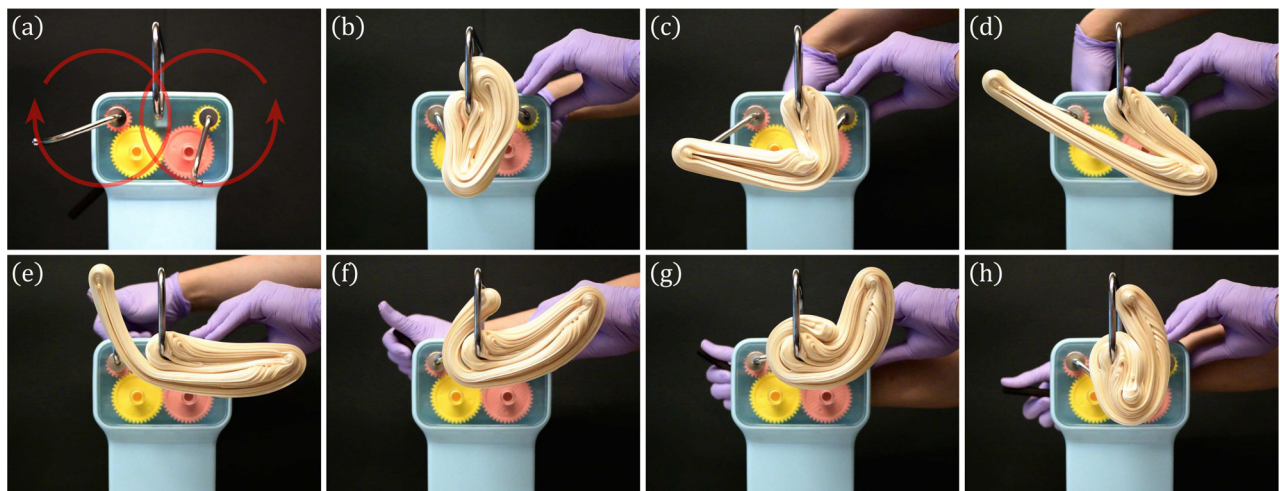
FIG. 3. Taffy pulling by a mechanical device. (a) Image of the toy taffy puller, consisting of two rotatable arms and a fixed hook. The red arrows exhibit the loci traversed by the ends of the arms and the directions in which the arms move. (b)–(d) Movement of the arms away from the hook, stretching the taffy. (e)–(h) Movement of the arms back toward the hook, folding the taffy onto itself. For (b)–(h), the time interval separating successive images is ~ 0.1 s.

fractional Maxwell gel (FMG) model, which comprises three parameters: a plateau modulus, a characteristic relaxation time, and a single power-law exponent.[11] The master curves for taffy of different flavors can all be described by the same FMG model, with a certain fixed value of the relaxation exponent. Scaling the master curves with the plateau modulus and relaxation time leads to their collapse onto a supermaster curve, signifying a more fundamental time–temperature–taffy superposition (TTTS) principle.

We also explore the viscoelastic response of lab-made model syrups composed of sucrose, fructose, and varying water contents, which exhibit plateau moduli and relaxation times similar to commercial taffy. This suggests that the rheology of the taffy at timescales comparable to the relaxation time is governed by its sugar content. Another supermaster curve can be obtained for syrups of various water contents. By using the two supermaster curves as upper and lower bounds, we investigate the impact of aeration and emulsification on taffy rheology by varying the extent of taffy-pulling. We show that this stretching and folding process progressively shift the linear viscoelastic response of the lab-made model taffy away from the syrup and toward that of commercial taffy. This evolution in the underlying viscoelastic spectrum is attributed to the broad size distribution of the inclusions (air bubbles and oil droplets) that are incorporated into the sugar syrup matrix during the taffy-pulling process.

II. PRELIMINARIES
A. Material preparation

The three materials considered in this study are commercial salt-water taffy, lab-made model syrup, and lab-made model taffy. The commercial taffy is a variety named "Assorted Salt Water Taffy" (Sweet Candy Company, Salt Lake City, UT). The primary ingredients of the commercial taffy include sucrose (table sugar), corn syrup, water, coconut oil, and soy lecithin, with additional minor ingredients including salt, food coloring, and flavoring. To estimate the unknown water content of the commercial taffy, we select and weigh five random samples before drying them in an oven at $60\,°C$ for 3 weeks. The water content $c_w = 3$ wt. % of the commercial taffy is estimated by subtracting the dry weight from the wet weight and dividing the result by the wet weight.

The model syrups are prepared using food-grade sucrose, fructose, and tap water. We combine 200 g of sucrose, 83 g of fructose, and ~ 60 g of water in a stainless-steel pot and cook the uncovered mixture on a hot plate at $200\,°C$ (corresponding to medium-high heat on a gas stove) until it reaches the desired c_w. The relative amounts of sucrose and fructose needed to make the syrups are obtained from an online taffy recipe.[12] The pot is occasionally swirled and rotated to distribute the heating as evenly as possible. Two common approaches for estimating c_w in confectionery practice include monitoring syrup temperature with a candy thermometer and the cold water test.[2] Instead, we employ a less common but more accurate method: monitoring the weight of the syrup over time until it decreases to the desired value, corresponding to the target c_w. Using a rather large amount of sucrose and fructose helps to minimize the error in measuring c_w.

The model taffy samples are prepared by pulling model syrups for at least 15 min either by hand or with a toy taffy puller (Chef'n Corporation).[8] We rely on a simple method for estimating the volumetric air content in the model taffy. A sample (syrup or taffy with the same prescribed value of c_w) is rolled into a long cylinder with a diameter of 6 mm and a length of at least 110 mm. After calculating the volume of each sample, we use an electronic balance to measure its mass and, thus, its mass density. Using ρ_s and ρ_t to represent the mass density of the syrup and taffy, respectively, the air content is calculated as $c_a = 1 - \rho_t/\rho_s$, expressed in vol. %. In some trials, 15 g of unsalted butter (assuming 80 wt. % fat), 12 g of coconut oil, or 12 g of vegetable oil (extracted from rapeseed, palm, and corn), with and without adding 3 g of soy lecithin as an emulsifying agent, are included in the recipe to examine the effect of emulsification on taffy rheology.

To minimize moisture absorption, all materials are wrapped with either wax paper or a silicone mat and are stored in a closed box containing silica-gel beads at room temperature before conducting experiments. Experiments are performed within a week after the arrival of the commercial taffy and 2 days after the preparation of the lab-made model syrups and taffy.

B. Visualization of bubbles and droplets

Since taffy is opaque, conventional light microscopy cannot be used to image its internal distributions of air bubbles and oil droplets. To address this issue, we immerse the sample (commercial or model taffy) for ~ 10 min in a 20 wt. % Pluronic F127 hydrogel, the yield stress of which is in the order of 100 Pa.[13] As the taffy sample swells in the gel, the bubbles and droplets are entrapped in the transparent Pluronic solution due to its yield stress, thus allowing them to be imaged. A SONY ILCE-6000 digital camera is used in conjunction with a Nikon SMZ1270 stereo microscope for capturing the images. This setup has a pixel resolution of $0.4\,\mu m$. Although the sizes of the air bubbles and oil droplets dispersed in the gel might be influenced over long timescales by Ostwald ripening and coalescence,[14] the effects of these processes are minimal in our brief visualization experiments as the bubbles and droplets are stabilized by the lecithin in the taffy and also by the very high shear viscosity of the unyielded Pluronic hydrogel.

We also employ x-ray micro-computed tomography[15,16] to non-destructively visualize the internal structure of the taffy. Before scanning, the taffy is securely mounted in a custom-made cylindrical sample holder. The scanning process is conducted with a Zeiss Xradia Versa 510 microscope, using the following settings for optimal scan quality: $0.4\times$ objective, 50 kV x-ray voltage, $80\,\mu A$ x-ray current, 2 s exposure time, and 801 projections for a complete revolution of the taffy sample. This configuration yields a voxel resolution of $(6.4\,\mu m)^3$. Subsequently, the three-dimensional model of the taffy is reconstructed utilizing the Imaris microscopy image analysis software (Oxford Instruments).

C. Rheological measurements

All rheological measurements of the various taffy and syrup samples are conducted using an ARES-G2 strain-controlled torsional rheometer (TA Instruments) installed with a cone-partitioned plate fixture.[17] This fixture comprises a cone with an angle of $5.73°$ and a plate partitioned into an inner disk of radius 5 mm and an outer ring of radius 12.5 mm. The inner disk is connected to the stress transducer, and the outer ring is mounted to the rheometer frame. Consequently, only the inner 5 mm radial portion of the sample contributes to the rheological measurement. The outer 7.5 mm annular portion of the excess sample functions as a protective layer, preventing

the central area from coming into contact with the environment and thus minimizing moisture absorption. The cone-partitioned plate offers an additional advantage: the sticky sample materials can simply be overfilled into the fixture without requiring precise trimming. The temperature is controlled by a forced convection oven (TA Instruments) with a precision of $\pm 0.1\,^\circ$C.

The main rheological test protocol used in the present study is the small amplitude oscillatory shear (SAOS) test.[18] The sample is subjected to a sinusoidal shear strain of amplitude γ_0 and frequency ω. The resulting complex modulus $G^*(\omega) = G'(\omega) + jG''(\omega)$ is measured, where $j = \sqrt{-1}$. The storage modulus G' characterizes the elastic (solid-like) behavior, and the loss modulus G'' characterizes the viscous (liquid-like) behavior. To ensure that G' and G'' are independent of γ_0, the SAOS measurement is repeated with at least two values of γ_0 across the entire frequency range of interest. For the testing temperature $T = 25\,^\circ$C, when the magnitude of G' becomes similar to that of G'' at high frequencies ($\omega > 10$ rad s^{-1}), a strain amplitude of $\gamma_0 = 0.01\%$ is used for the SAOS measurement; a larger $\gamma_0 = 0.1\%$ does not influence the results. At lower frequencies and for higher temperatures, a strain amplitude of $\gamma_0 = 1\%$ is used; here, an increase to $\gamma_0 = 2\%$ has no discernible impact on the measurement results. For SAOS, another important measurable quantity is the phase angle $\delta = \tan^{-1}(G''/G')$. The particular values $\delta = 0$ and $\delta = \pi/2$ are expected for a purely elastic solid and a purely viscous liquid, respectively.

We also employ stress relaxation and creep tests in this study. During a stress relaxation test, a small step shear strain γ_0 is applied to the sample, and the stress response $\sigma(t) = G(t)\gamma_0$ is monitored over time, where $G(t)$ is the relaxation modulus. During a creep test, a small step increase in the imposed shear stress σ_0 is applied, and the strain response $\gamma(t) = J(t)\sigma_0$ is monitored, where $J(t)$ is the creep compliance. In the linear viscoelastic limit, $G(t)$ and $J(t)$ are directly related to $G'(\omega)$ and $G''(\omega)$ via Fourier transformation.[19]

D. The FMG model

A wide range of mathematical models based on distinct underlying physics have been developed to describe the linear viscoelastic properties of different classes of materials. These models predict specific functional forms of $G'(\omega)$, $G''(\omega)$, $G(t)$, and $J(t)$ that can be fitted to the experimental data, enabling rheologists to infer the mechanisms governing the observed viscoelastic response of soft materials such as foods and consumer products and gain insights into their structure. In the context of taffy rheology, we employ the fractional Maxwell gel (FMG) model

$$\sigma(t) + \tau_c^\alpha \frac{d^\alpha \sigma(t)}{dt^\alpha} = G_c \tau_c^\alpha \frac{d^\alpha \gamma(t)}{dt^\alpha}, \tag{1}$$

where G_c is the plateau modulus, τ_c is the characteristic relaxation time, and $0 \leq \alpha \leq 1$ is the power-law exponent characterizing the limiting low-frequency response of the complex modulus. The distinctive combination of these three independent variables occurring on the right-hand side of (1) can also be written as a single "quasi-property" $\mathbb{V} = G_c \tau_c^\alpha$ with units of Pa s$^\alpha$.[20,21] The operator d^α/dt^α is the Caputo fractional derivative, a generalization of differentiation to noninteger orders; we refer readers to the articles by Song et al.,[11] Bonfanti et al.,[22] and Rathinaraj et al.[23] for in-depth analyses of related concepts in fractional rheology. In brief, the FMG model predicts the following SAOS response:

$$\frac{G'(\omega)}{G_c} = \frac{(\omega\tau_c)^{2\alpha} + (\omega\tau_c)^\alpha \cos(\pi\alpha/2)}{1 + (\omega\tau_c)^{2\alpha} + 2(\omega\tau_c)^\alpha \cos(\pi\alpha/2)}, \tag{2}$$

$$\frac{G''(\omega)}{G_c} = \frac{(\omega\tau_c)^\alpha \sin(\pi\alpha/2)}{1 + (\omega\tau_c)^{2\alpha} + 2(\omega\tau_c)^\alpha \cos(\pi\alpha/2)}. \tag{3}$$

In Fig. 4, we illustrate the predicted SAOS response of the FMG model with varying values of α. The FMG framework provides a compact description of the multiscale relaxation processes that are present in many complex gels and foodstuffs. Detailed comparisons between microscopic computer simulations, x-ray scattering, and rheological characterization[24,25] show that the FMG model captures the dynamics of a fractal-like microstructure and a broad relaxation spectrum in terms of just three parameters: G_c, τ_c, and α. The FMG model has three important limiting cases. For $\alpha = 1$, the model reduces to the Maxwell model, the simplest model for describing viscoelastic fluids,

$$\frac{G'(\omega)}{G_c} = \frac{(\omega\tau_c)^2}{1 + (\omega\tau_c)^2}, \tag{4}$$

$$\frac{G''(\omega)}{G_c} = \frac{\omega\tau_c}{1 + (\omega\tau_c)^2}. \tag{5}$$

For $0 < \alpha \leq 1$ and $\omega\tau_c \gg 1$, the model approaches a purely elastic response with a plateau modulus satisfying the following criteria:

$$G'(\omega) \rightarrow G_c, \tag{6}$$

$$G''(\omega) \rightarrow 0. \tag{7}$$

For $\omega\tau_c \ll 1$, the FMG model reduces to the Scott Blair spring pot model,[21] which exhibits a power-law frequency response of the following form:

$$G'(\omega) = G_c(\omega\tau_c)^\alpha \cos(\pi\alpha/2), \tag{8}$$

$$G''(\omega) = G_c(\omega\tau_c)^\alpha \sin(\pi\alpha/2). \tag{9}$$

The phase angle predicted by the spring pot is $\delta = \pi\alpha/2$, a constant. This result can also be written in the form of the "critical gel" model described by Winter et al.[20,26] The spring pot can compactly describe materials with a fractal-like underlying microstructure spanning a broad range of length scales.[25] This distribution of length scales contributes to a broad range of relaxation modes in the material, leading to self-similar relaxation behavior with time. Representative materials that can be described by the spring pot model include cheese,[27,28] bread dough,[29] and chewing gum,[30] which contain microstructures such as polydisperse polymer chains, air bubbles, and oil droplets, all of which give rise to a broad distribution of relaxation timescales in those materials.

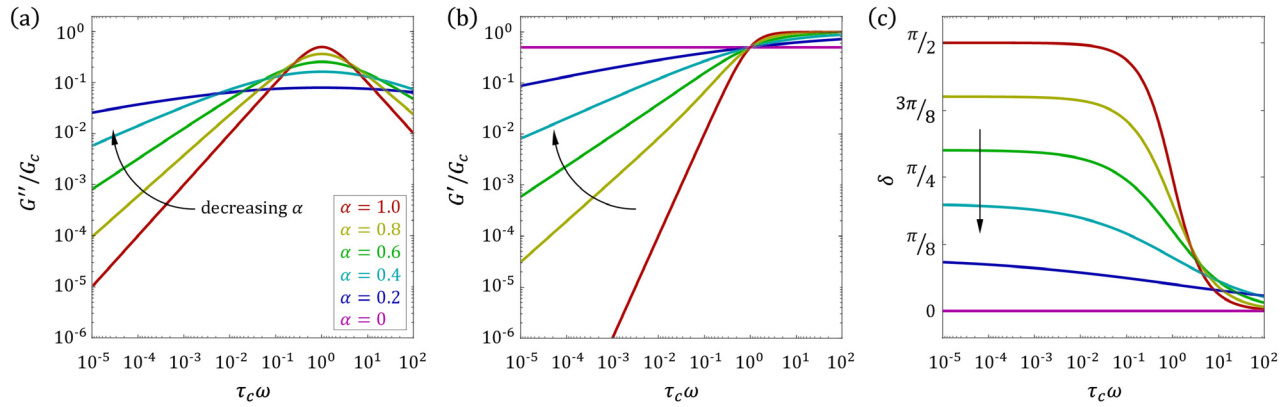In addition to SAOS, the stress relaxation and creep compliance, as described by the FMG model, are

$$G(t) = G_c E_{\alpha,1}(-z) \tag{10}$$

and

$$J(t) = \frac{1}{G_c}\left(1 + \frac{z}{\Gamma(1+\alpha)}\right), \tag{11}$$

where $z = (t/\tau_c)^\alpha$, $E_{\alpha,1}$ is the two-parameter Mittag–Leffler function, and Γ is the gamma function.[23] The relations in (10) and (11) will be

FIG. 4. Small amplitude oscillatory shear (SAOS) responses as predicted by the Fractional Maxwell Gel (FMG) model [(2) and (3)] with different power-law exponents α. (a) The scaled loss modulus G''/G_c as a function of the dimensionless angular frequency $\tau_c\omega$, where G_c is the plateau modulus and τ_c is the relaxation time. For $\alpha = 0$, $G''(\omega) \to 0$ and the response is purely elastic. Hence, the curve for $\alpha = 0$ is not shown in the log–log plot. (b) The scaled storage modulus G'/G_c as a function of $\tau_c\omega$. (c) The phase angle δ as a function of $\tau_c\omega$, with $\delta = \tan^{-1}(G''/G')$. The arrows in (a)–(c) represent the direction of decreasing α.

used to verify the predictions of the FMG model after regression to the SAOS data of the taffy.

E. Time–temperature superposition

The time–temperature superposition principle allows construction of master curves that apply over wide ranges of the frequency ω by shifting self-similar curves of the dynamic moduli G' and G'' obtained at different temperatures horizontally along the frequency axis.[9] The shifting is performed by multiplying ω by a factor a_T depending on the test temperature T and the selected reference temperature T_r.

If a material follows the principles of time–temperature superposition, then it can be concluded that the underlying stress relaxation mechanisms within the material all respond to temperature similarly. In such a case, the material is said to be thermorheologically simple. If two materials have distinct underlying molecular interactions or structural characteristics, then their viscoelastic properties will typically vary with temperature differently, leading to two distinct sets of shift factors a_T. Conversely, if two materials have similar values of a_T over a range of temperatures, then it can be concluded that the same molecular interactions or structural traits govern their rheological behavior within that range of temperatures. In such a case, the two materials are said to be thermorheologically similar.

The relationship between a_T and T at a chosen reference temperature T_r (in this study, $37\,°C$) can be described using the Arrhenius model,[31–33] which reads

$$\ln a_T = \frac{E_A}{R}\left(\frac{1}{T} - \frac{1}{T_r}\right), \qquad (12)$$

where T and T_r are measured on the Kelvin scale (K). The terms E_A and R are the activation energy for flow and the universal gas constant, respectively. In rheology, E_A can be interpreted as the amount of energy required to bring a material from one rheological state to another. We note that the Williams–Landel–Ferry (WLF) model, which contains two empirical fitting parameters, can quantitatively describe the evolution of a_T over a larger range of T.[34–36] However,

since our study focuses on the relatively narrow temperature range of $25–45\,°C$, we have opted for the simpler Arrhenius model, adhering to the principle of Occam's razor.

III. RESULTS AND DISCUSSION
A. Thermorheological properties of commercial taffy

1. The rheological effects of temperature

The SAOS results for a commercial blueberry-flavored taffy obtained at various temperatures T are presented in Fig. 5(a). The two components of the complex modulus are very close to parallel across three decades of the oscillatory frequency ω, which is reminiscent of the self-similar relaxation behavior of a critical gel.[20,26] For any given $T > 25\,°C$, the measured loss modulus G'' is greater than the storage modulus G' at all imposed oscillation frequencies ω, indicating that the taffy exhibits a more dissipative liquid-like characteristic than purely elastic solid-like behavior. However, at the lowest test temperature of $T > 25\,°C$, G' and G'' intersect at a sufficiently large value of ω, signifying a crossover toward a predominantly elastic response.[10] The taffy transitions from a dissipative, critical gel-like state to an elastic, solid-like state. The propensity of taffy to undergo such a transition indicates that its underlying material structure is predominantly amorphous and lacks the long-range order characteristic of crystalline materials. This observation is consistent with the confectionery practice of candy-making, in which syrup containing crystallization inhibitors like glucose or fructose is added, and the cooked sugar mixture is rapidly cooled to prevent crystallization.[37,38]

By applying the time–temperature superposition principle, we can construct a master curve at the reference temperature of $T_r > 37\,°C$ [Fig. 5(b)]. The presence of a time–temperature superposition principle in this context points to another piece of evidence for the absence of crystallization. The shift factors a_T are very well described by the Arrhenius model (12), yielding $E_A/R = 2.24 \times 10^4$ K. The master curve is well captured by the FMG model [(2) and (3)], with a power-law exponent $\alpha = 0.88$, rubbery plateau modulus $G_c = 8.7$ MPa, and characteristic relaxation time
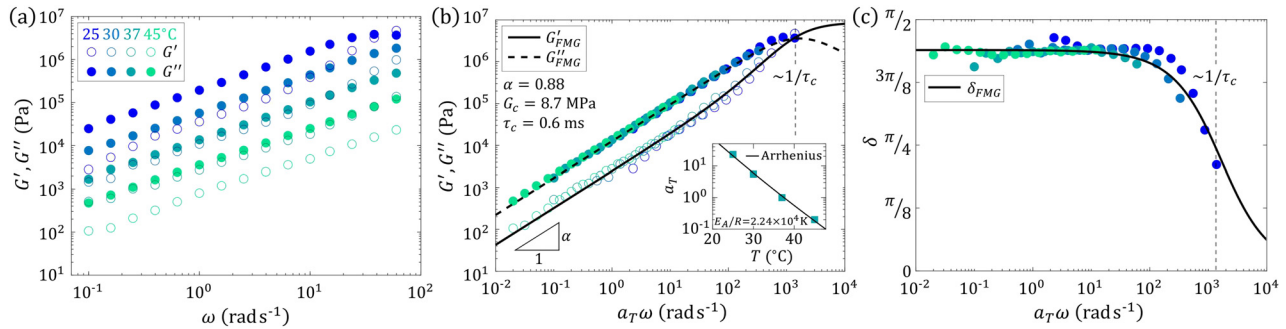
FIG. 5. SAOS test results for a commercial blueberry-flavored taffy. (a) Storage and loss moduli G' and G'' as functions of the angular frequency ω at different temperatures T. For $T = 25\,°C$ and $\omega > 10$ rad s^{-1}, a strain amplitude of $\gamma_0 = 0.01\%$ is used for the SAOS measurement. Otherwise, a strain amplitude of $\gamma_0 = 1\%$ is used. (b) A master curve formed by horizontally shifting G' and G'' measured at different temperatures T to corresponding values of frequency obtained at the reference temperature $T_r = 37\,°C$, showing G' and G'' as functions of the reduced frequency $\omega_r = a_T\omega$. The black solid and broken lines represent the fit to the three parameter FMG model [(2) and (3)]. The inset figure shows the horizontal shift factor a_T as a function of T; the black line within the inset is the fit to the Arrhenius model (12). (c) The phase angle δ as a function of ω_r. The black line is the prediction of the FMG model [(2) and (3)].

$\tau_c = 0.6$ ms determined at the reference temperature $T_r > 37\,°C$. For reduced frequencies $\omega_r = a_T\omega < 100$ rad s^{-1}, the taffy is a critical gel-like material and shows self-similar, power-law relaxation behavior over four decades of frequency, which can be compactly described by the Scott Blair spring pot [(8) and (9)]. This observation suggests the presence of a fractal-like microstructure in the taffy, contributing to a very broad range of relaxation modes. Given that time–temperature superposition applies, we can conclude that taffy is thermorheologically simple for $25\,°C \le T \le 45\,°C$; we expect that common underlying molecular interactions or structural characteristics govern the relaxation modes present in the taffy within this specific temperature range. Figure 5(c) shows the phase angle δ as a function of ω_r. The phase angle δ exhibits a plateau at low reduced frequencies with a constant value of $\pi\alpha/2$, as described by the spring pot model. The magnitude of the phase angle decreases monotonically as ω_r approaches and exceeds $1/\tau_c$, showing that the taffy becomes increasingly rubbery at short deformation timescales.

In Fig. 6(a), we present the stress relaxation test results obtained at $T = 37\,°C$ for the blueberry taffy. The relaxation modulus $G(t)$ exhibits a continuous power-law decay with elapsed time t when a

step shear strain of magnitude $\gamma_0 = 1\%$ is applied at time $t = 0$, which is again accurately predicted by the FMG model (10). In Fig. 6(b), we show results for the corresponding creep compliance. The creep compliance $J(t)$ of the taffy increases in a power-law manner with time t after a step shear stress $\sigma_0 = 500$ Pa is applied. This trend is also well predicted by the FMG model (11) without adjusting the three material constants, confirming that the model effectively describes the linear rheology of taffy over a range of deformation histories.

2. The rheological effects of minor ingredients

The master curves obtained for different flavors of taffy can be constructed using the same shift factors a_T, indicating that the various flavors of commercial taffy are thermorheologically similar. The master curve obtained for each taffy flavor can be fitted by the FMG model using the same values of $\alpha = 0.88$ and $G_c = 8.7$ MPa found for the blueberry taffy, but with a weakly flavor-dependent relaxation time $0.5 \le \tau_c \le 1$ ms. These observations indicate that the rheology of taffy is largely insensitive to minor ingredients like flavorings and colorings, slight variations in the amounts of major ingredients added to it, and slight variations in the taffy-pulling process.

On scaling G' and G'' with G_c, and scaling the reduced frequency $\omega_r = a_T\omega$ of each taffy with the timescale τ_c, the SAOS data for taffy of various flavors all collapse onto a single, universal master curve. Figure 7 illustrates this supermaster curve for blueberry, banana, grape, chocolate, and mint-flavored taffy, encompassing all the rheological features previously discussed for the blueberry taffy in Fig. 5(b). This observed universality across different flavors of taffy points to a more fundamental time–temperature–taffy superposition (TTTS), or time–temperature–flavor superposition (TTFS), which extends beyond the traditional time–temperature superposition. TTTS is analogous to the time–pH and time–salt superpositions observed in polyelectrolytes,[39–41] the time–concentration superposition observed in worm-like micellar solutions,[42] the time–connectivity superposition observed in soft colloidal gels,[24,25] and the time–water content superposition observed in bread doughs.[43] We thus conjecture that minor ingredients and slight variations in taffy recipes primarily affect local interactions within the underlying microstructure of the taffy without
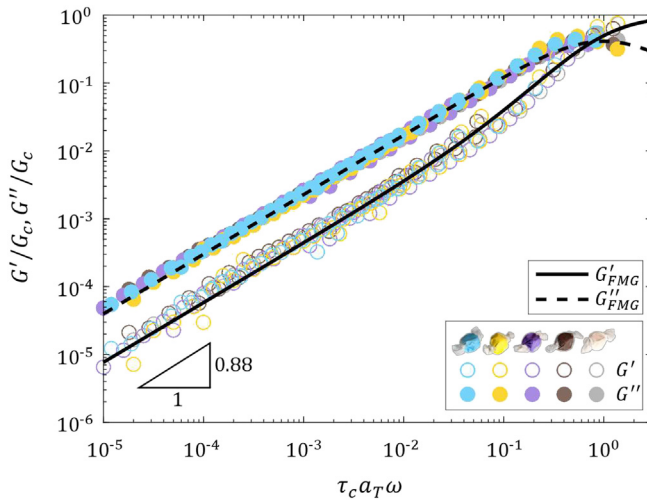

FIG. 6. (a) Stress relaxation test result for a commercial blueberry-flavored taffy showing the relaxation modulus $G(t)$ as a function of time t following an applied step shear strain γ_0 at a test temperature $T = 37\,°C$. (b) Creep test result showing the creep compliance $J(t)$ as a function of time t under an applied step shear stress σ_0 at $T = 37\,°C$. The black lines in (a) and (b) represent the corresponding prediction of the FMG model [(10) and (11)].

FIG. 7. A supermaster curve formed by nondimensionalizing the master curves of the blueberry, banana, grape, chocolate, and mint flavored taffy and showing the scaled dynamic moduli G'/G_c and G''/G_c as functions of the dimensionless reduced frequency $\tau_c \omega_r = \tau_c a_T \omega$. The black solid and broken lines represent the fit to the FMG model [(2) and (3)].

FIG. 8. A supermaster curve formed by nondimensionalizing the master curves of lab-made model syrups of different water contents c_w, showing the scaled dynamic moduli G'/G_c and G''/G_c as functions of the dimensionless reduced frequency $\tau_c \omega_r = \tau_c a_T \omega$. Data points corresponding to the measurement of G', where $G' < 0.001 G''$ and below the resolution limit of the rheometer have been excluded. The black solid and broken lines are the fit to the linear Maxwell model [(4) and (5)]. The inset shows an image of a $c_w = 8$ wt. % syrup.

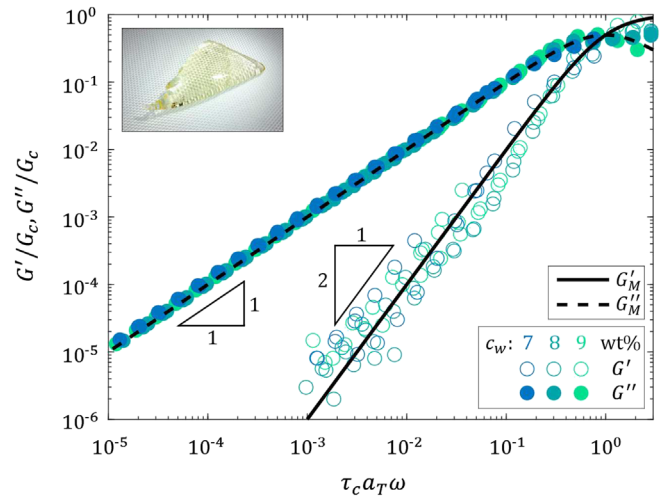substantially altering the fundamental nature of the interactions and structural properties of the taffy.

B. Thermorheological properties of model syrup and taffy

1. The rheological effects of sugar and water

Granted that the effects of minor ingredients like flavorings and colorings can be neglected, we examine how variations in primary ingredients influence the rheological properties of taffy. These major ingredients typically consist of sugars (sucrose, glucose, and fructose), emulsifiers (lecithin), water, oil, and air. Since sugars and water are the most fundamental components of taffy, we will first examine their influence on the material's rheological behavior. In particular, we consider the rheology of several lab-made model syrups solely made of sucrose, fructose, and water (Fig. 8 inset).

Like commercial taffy, model syrups of water content $c_w = 7$, 8, and 9 wt. % adhere to the time–temperature superposition principle. Their shift factors a_T can be described by the Arrhenius model (12), and their master curves can be described using the classical Maxwell model [(4) and (5)], a limiting case of the FMG model [(2) and (3)] arising for $\alpha = 1$. The fitting parameters are listed in Table I. The activation energies E_A for the three syrups all are of similar magnitude. Within the temperature range of $25\,°C \leq T \leq 45\,°C$, the values of $\ln a_T$ for the syrups are essentially indistinguishable from those for the commercial taffy [Fig. 5(b), inset]. This observation indicates that the three syrups are thermorheologically similar to the commercial taffy; their rheological properties all depend similarly on temperature.

The flow activation energy E_A decreases as the water content c_w in the syrup increases. A comparable trend is observed for the Maxwell model parameters: the characteristic modulus G_c and the characteristic timescale τ_c exhibit a systematic decrease as c_w increases. This observation aligns with the understanding that water is an effective plasticizer of

the amorphous sugar matrix. Water can significantly soften food materials by shielding their intra- and inter-molecular hydrogen bonds and dipole–dipole interactions.[44] Furthermore, the values of G_c and τ_c for the syrups share the same order of magnitude as those of commercial taffy, implying that the observed rubbery behavior of in taffy at high deformation rates is due to its sugar content.

The linear viscoelastic response of all the three syrups can be described by the Maxwell model. This allows us to create a single supermaster curve for a range of water contents c_w (Fig. 8). The sugar syrup food matrices thus obey a time–water content superposition principle (as also observed in other soft food materials like bread dough[43] as well as in hydrogels[45]). If desired, the data can be shifted to a reference water content using horizontal and vertical shift factors a_w and b_w, respectively. However, for clarity, given the limited range of water contents considered, we simply report the relevant values of τ_c and G_c as a function of the water content c_w in Table I. Over a wide range of intermediate frequencies, the storage and loss moduli exhibit Maxwell-like responses with $G' \propto \omega^2$ and $G'' \propto \omega$, respectively. In the low-frequency regime ($\tau_c a_T \omega < 0.01$), $\delta \approx \pi/2$, meaning that the syrups display rheological properties very close to those of a purely viscous liquid. Nonetheless, the observation that α is insensitive to c_w

TABLE I. Arrhenius and Maxwell model parameters for lab-made model syrups of various water contents c_w.

c_w (wt. %)	7	8	9
E_A/R (K)	2.24×10^4	2.09×10^4	1.95×10^4
G_c (MPa)	11.0	9.5	7.5
τ_c (ms)	0.60	0.25	0.20

suggests that water content is not the main factor governing the self-similar relaxation behavior of commercial taffy. Moreover, on comparing the supermaster curves in Figs. 7 and 8, it becomes apparent that varying the composition of sugar and water alone cannot account for the broad and pronounced increase in the elastic storage modulus at intermediate frequencies and the observed power-law exponent of $\alpha = 0.88$ for commercial taffy. Another possible key to taffy rheology lies in presence of air, oil, and emulsifier.

2. The rheological effects of aeration

To investigate the effect of aeration, we intentionally pulled the $c_w = 8$ wt. % model syrup with a toy taffy puller (Fig. 3) for more than 15 min, which is at least five times the pulling duration for commercial taffy.[3,4] The outcome is an overaerated model taffy with an estimated air content of $c_a = 30$ vol. % (Fig. 9 inset). Such a value is comparable to nougats (30–40 vol. %) but lower than marshmallows (68–75 vol. %).[46] In contrast to the yellowish, transparent appearance of the model syrup (Fig. 8 inset), the overaerated taffy exhibits a white appearance characteristic of aerated food foams and emulsions.[47] On top of aeration, another possible mechanism that could have caused the coloration of the model taffy is crazing, the whitening of amorphous polymers when subjected to sufficiently strong tensile stress.[48–50] However, the molecular weights of sucrose and fructose are much smaller than those of typical long-chained polymers like polystyrene and polymethyl methacrylate; crazing is therefore considered unlikely for the model taffy.

In Fig. 9(a), we show the master curve at the reference temperature $T_r = 37\,^\circ$C for the overaerated model taffy, which features a characteristic 'shoulder' in G' in the range 1 rad s^{-1} $< \omega_r = a_T\omega < 100$ rad s^{-1} that the FMG model cannot capture. However, for $\omega_r < 1$ rad s^{-1}, G' and G'' exhibit a broad critical gel-like response [(8) and (9)] with a noninteger value $\alpha = 0.75$ of the power-law exponent. This observation suggests that aeration plays a significant role in altering taffy rheology over a wide range of timescales associated with

handling and chewing. On the other hand, for $\omega_r > 100$ rad s^{-1}, G' and G'' can again be compactly described using the Maxwell model [(4) and (5)] with $G_c = 60$ MPa and $\tau_c = 0.2$ ms. In Fig. 9(b), we further show how the phase angle δ of the overaerated model taffy varies as a function of ω_r. Two distinct regimes can again be identified: a spring-pot-like regime with a constant value of $\delta \approx 3\pi/8$ corresponding to $\omega_r < 1$ rad s^{-1}, and a Maxwell-like regime with δ progressively decaying from $\pi/2$ towards zero corresponding to $\omega_r > 100$ rad s^{-1}.

The foregoing observations lead us to suggest that the rheology of taffy in the high-frequency regime is dictated primarily by its sugar content. Aeration governs the power-law response observed in the viscoelastic moduli at low frequencies, potentially due to the formation of a distributed network of air bubbles within the material, which leads to a fractal-like porous microstructure, contributing to the self-similar viscoelastic relaxation behavior of taffy. However, the air bubbles would exhibit different deformation time scales at varying temperatures due to the variation of surface tension and viscosity with temperature; also, taffy is thermorheologically similar to the model sugar syrups (see Sec. III B 1), which do not contain air bubbles. The thermorheological simplicity of taffy likely does not originate from the bubbles but from the porous sugar scaffold that forms the weakly viscoelastic matrix suspending the inclusions.

3. The rheological effects of emulsification

To investigate the effects of emulsification, we prepare model syrups with varying oil and lecithin contents. We then create a set of model taffy samples by manually pulling the syrups (Fig. 2). Since these model syrups contain oils, the pulling process not only aerates the taffy but also emulsifies the oil within it. After at least 15 min of manual pulling, the air content is estimated to be $c_a = 3$ vol. %. The lower air content is also evident if we observe the color of the taffy [Fig. 10(a) inset], which appears more yellowish than the white overaerated model taffy [Fig. 9(a) inset].
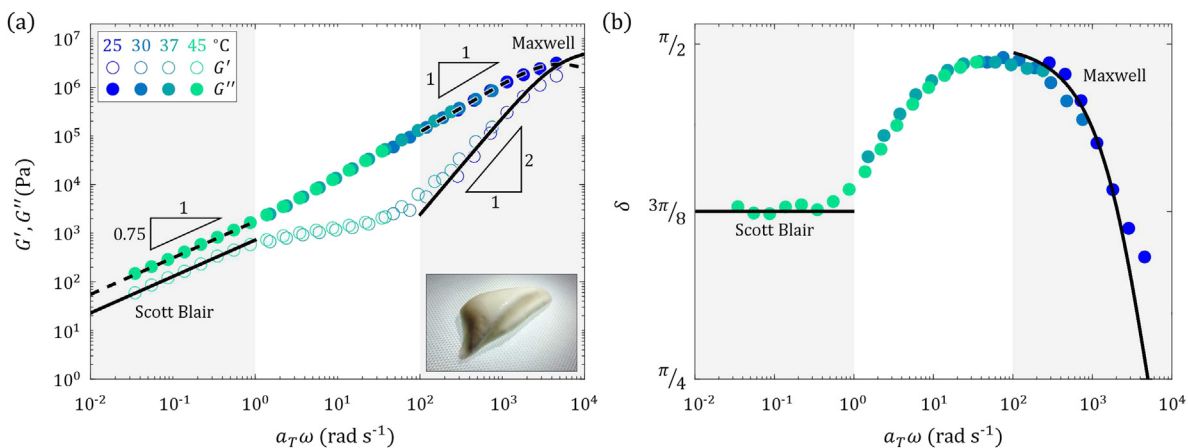
FIG. 9. (a) A master curve showing the dynamic moduli G' and G'' as functions of the reduced frequency $\omega_r = a_T\omega$ for an overaerated model taffy at the reference temperature $T_r = 37\,^\circ$C. The black solid and broken lines on the left-hand side represent the fit to the Scott Blair spring pot model [(8) and (9)], while those on the right-hand side represent the fit to the Maxwell model [(4) and (5)]. The inset in (a) is an image of an overaerated taffy of air content $c_a = 30$ vol. % made from the $c_w = 8$ wt. % model syrup (Fig. 8, inset). (b) The phase angle δ as a function of ω_r. The black solid line on the left-hand side represents the response predicted by the spring pot model, while that on the right-hand side represents the response predicted by the Maxwell model.
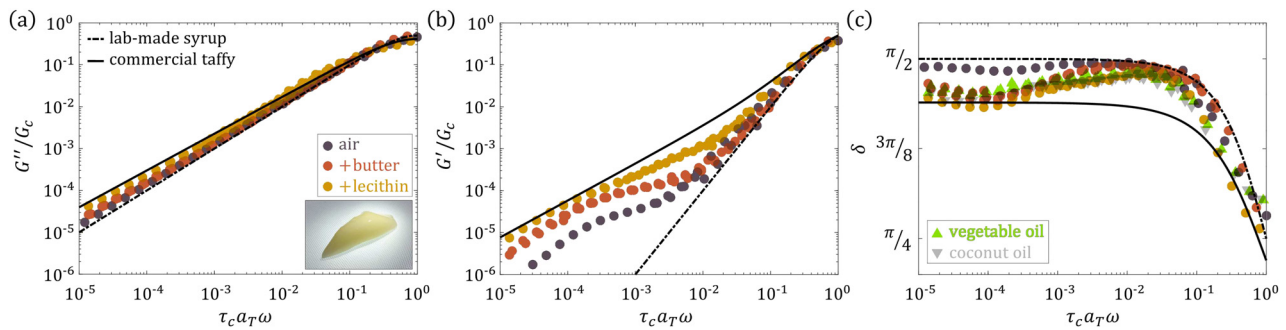
FIG. 10. (a) The scaled loss modulus G''/G_c as a function of the dimensionless reduced frequency $\tau_c\omega_r = \tau_c a_T\omega$ for three different model taffies: one without butter, one with butter added, and one with both butter and lecithin added. The inset image shows a taffy with final air content $c_a = 3$ vol. % made from the $c_w = 8$ wt. % model syrup (Fig. 8, inset). (b) The evolution in the scaled storage modulus G'/G_c as a function of $\tau_c\omega_r$ for the three model taffies. (c) The evolution in the phase angle δ as a function of $\tau_c\omega_r$ for the three model taffies and two additional taffies, with lecithin added and vegetable oil or coconut oil replacing butter. For (a)–(c), the black solid lines represent the fit to the FMG model [(2) and (3)] to the commercial taffies; the broken lines represent the fit to the Maxwell model [(4) and (5)] to the lab-made model syrups.

Figures 10(a) and 10(b) show the scaled loss and storage moduli G''/G_c and G'/G_c (respectively) for three different model taffy samples: one without butter added, another with butter added, and a third with both butter and lecithin added. The FMG model fits for the commercial taffy and the model sugar syrups, as shown previously in Figs. 6 and 7, are also included for comparison. Notably, aeration and emulsification primarily affect G' but not G''. The effect of these processes is to make the taffy increasingly viscoelastic.

As shown in Fig. 10(b), the model taffy without butter added (which is thus only aerated) has a characteristic shoulder in G' around $\tau_c\omega_r = \tau_c a_T\omega = 0.01$, similar to that observed for the overaerated taffy for 1 rad s^{-1} < ω_r < 100 rad s^{-1} in Fig. 9(a). For $\tau_c\omega_r > 0.01$, the trend in G'/G_c is well described by the Maxwell model, indicating that at higher oscillatory frequencies, the rheology resembles that of the model syrups and is governed by the sugar content. For $\tau_c\omega_r < 10^{-4}$, the scaled elastic modulus G'/G_c for the butter-free taffy follows a power law, signifying self-similar relaxation behavior caused by aeration alone. However, the power-law exponent α can be estimated by regression to be 0.97, significantly larger than the measured value 0.75 for the overaerated model taffy [Fig. 9(a)]. This difference can be attributed to the much lower value of c_a for the manually-pulled taffy relative to that of the overaerated taffy. The best-fit value $\alpha = 0.97$ is also larger than the measured value of 0.88 for commercial taffy, which we hypothesize is due to the absence of oil droplets in the butter-free taffy.

When butter is added to the lab-made taffy, the low frequency regime of the scaled elastic modulus G'/G_c now follows a power-law trend with $\alpha = 0.93$, more closely following the FMG model. This can more clearly be seen using the representation in Fig. 10(c), which highlights the low-frequency asymptotic plateau in the phase angle δ, which approaches $\pi\alpha/2$. This signifies that the rheology of the model taffy becomes more similar to commercial taffy at low frequencies. This change can be attributed to the introduction of oil droplets to the taffy, as it affords a broader range of length scales for microstructures dispersed within the weakly viscoelastic sugar scaffold. Adding lecithin to such a taffy can further lower the interfacial tension of the dispersed air bubbles and oil droplets, enabling them to break into smaller sizes while suppressing their subsequent coalescence during the taffy-pulling process. Accordingly, the relaxation exponent decreases to

$\alpha = 0.89$, and G'/G_c moves even closer to the $\alpha = 0.88$ value of commercial taffy; the rheology of the model taffy now appears to be even more similar to that of commercial taffy.

To test how the oil type in a taffy recipe might alter the rheology of the taffy, we replace butter with coconut and vegetable oils for two additional batches of model taffies. Lecithin is also incorporated for stabilization purposes. According to the U.S. Department of Agriculture, typical butter consists of 45.6 wt. % saturated fat, 16.9 wt. % mono-unsaturated fat, and 2.5 wt. % polyunsaturated fat.[51] Coconut oil contains 82.5 wt. % saturated fat, 6.3 wt. % mono-unsaturated fat, and only 1.7 wt. % polyunsaturated fat.[52] In contrast, a typical vegetable oil (e.g., rapeseed oil) has only 6.6 wt. % saturated fat, 62.6 wt. % mono-unsaturated fat, and 25.3 wt. % polyunsaturated fat.[53] The distinct fatty acid compositions of butter, coconut, and vegetable oils result in their unique rheological properties at different temperatures, as evidenced by the common understanding that butter and coconut oil are solid at room temperature while vegetable oil remains liquid. Figure 10(c) shows the evolution of the phase angle δ for all the model taffies as functions of $\tau_c\omega_r$. The δ values for the taffies made with coconut and vegetable oils as obtained from their master curves are virtually indistinguishable from those made with butter, from which we conjecture that the linear viscoelasticity of taffy is insensitive to the oil type in a taffy recipe and the physical state of the pure oil (whether liquid or solid), at least in the temperature range of $25\,°C \leq T \leq 45\,°C$.

It is noteworthy that thermorheologically simple and self-similar relaxation behaviors similar to taffy have been observed for toffee, a popular unaerated confection made by caramelizing sugar with butter or condensed milk.[54] A visual inspection of the reported data shows that the power-law exponent for toffee[55] is on par with the obtained $\alpha = 0.75$ value for the overaerated model taffy. Toffee recipes typically contain 8–10 wt. % of water, 45–55 wt. % of sucrose, 40–50 wt. % of butter, 0.25–0.45 wt. % of lecithin, and other minor ingredients like salt and vanilla extract.[54] Assuming that the fat content of butter is 80 wt. %, the fat content in toffee is 32–40 wt. %, corresponding to roughly 32–40 vol. %. This value is on par with the volumetric air content $c_a = 30$ vol. % of the overaerated model taffy. This suggests that despite the very different rheological properties of oil and air, they likely have the same influence on the resulting rheology of sugar-based confections. In turn, this suggests that the interfacial properties of the

polydispersed inclusions (oil droplets and air bubbles) determine the ultimate linear viscoelastic behavior of a confection.

C. Size distribution of air bubbles and oil droplets

The self-similar relaxation behavior we observed for the various commercial and lab-made taffy samples considered so far implies that the air bubbles and oil droplets dispersed in the weakly viscoelastic sugar scaffold exhibit a nominally self-similar distribution spanning various length scales. To support this statement, we probe the size distribution of the immiscible inclusions (air bubbles and oil droplets) in the taffy. In Fig. 11(a), we present an example image for the model taffy with vegetable oil and lecithin added, showing a broad distribution of inclusion sizes. Figure 11(b) further shows the size distributions measured for the model taffy and a mint-flavored commercial taffy. Both distributions are well described by a lognormal distribution, the probability density of which can be expressed as

$$f(x) = \frac{1}{xs\sqrt{2\pi}} \exp\left(-\frac{(\ln(x/\langle x\rangle))^2}{2s^2}\right), \tag{13}$$

where $x > 0$ is the distributed variable, $\langle x\rangle$ is the log-weighted mean value of x, and s is the shape parameter. According to Kolmogorov's theory of successive fragmentation,[56] the observation that the sizes of

(a)

(b)

FIG. 11. (a) By swelling the taffy in a hydrogel with a weak yield stress, inclusions (air bubbles and oil droplets) within the taffy can be observed using a conventional stereo microscope. The zoomed-in image shows that the inclusions in a lab-made model taffy with vegetable oil and lecithin added assume a broad range of sizes. (b) Inclusion size distributions of the lab-made taffy (upper plot, sample size $n = 733$) and a mint-flavored commercial taffy (lower plot, $n = 1339$). The statistics can be described using the lognormal distribution (solid black lines) given by (13). The 95% confidence intervals of the shape factor s for the two lognormal distributions overlap, meaning that the two distributions are statistically indistinguishable.

the inclusions follow a lognormal distribution suggests that the probability of breaking each parent inclusion into a given number of offspring inclusions is independent of the size of the parent inclusion during taffy-pulling. Furthermore, the two lognormal distributions have the same shape parameter s (to within 95% confidence limits), meaning that the size distributions of the inclusions of the two taffy samples considered are statistically indistinguishable. This finding aligns with our previous observation that the two samples exhibit similar linear viscoelastic properties (Fig. 10).

As evidenced by the lognormal fits, the inclusions are of broadly distributed sizes. According to the Palierne model for viscoelastic emulsions, inclusions of different sizes and interfacial tensions in a viscoelastic matrix can introduce new relaxation modes. Adding up these individual relaxation modes would result in a broad relaxation spectrum.[57–61] For a viscoelastic emulsion composed of a matrix phase (e.g., the sugar matrix characterized by Fig. 8) with complex modulus $G_M^*(\omega)$ and an inclusion phase with complex modulus $G_I^*(\omega)$, the resulting complex modulus $G_E^*(\omega)$ of the viscoelastic emulsion can be expressed as

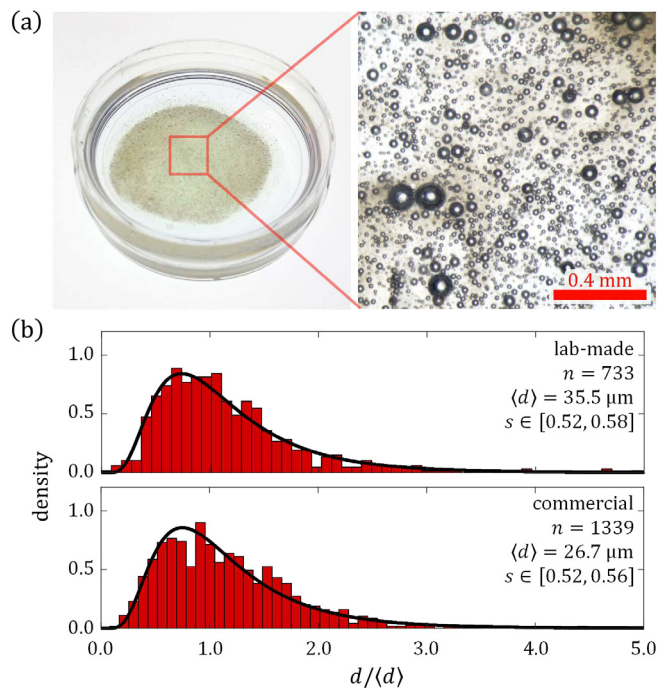$$G_E^* = \frac{1 + 3\sum_i \phi_i H_i}{1 - 2\sum_i \phi_i H_i} G_M^*, \tag{14}$$

where H_i is given by

$$H_i = \frac{\frac{8\sigma}{d_i}(2G_M^* + 5G_I^*) + (G_I^* - G_M^*)(16G_M^* + 19G_I^*)}{\frac{80\sigma}{d_i}(G_M^* + G_I^*) + (2G_I^* + 3G_M^*)(16G_M^* + 19G_I^*)}. \tag{15}$$

In Eq. (14), ϕ_i is the volume fraction of inclusions of diameter d_i; the total volume fraction of the inclusion phase is $\phi = \sum_i \phi_i$. In Eq. (15), σ is the interfacial tension between an inclusion and the matrix. The influence of the interfacial dilatational and shear properties between the inclusions and the matrix is assumed to be insignificant in this version of the model.[61]

The Palierne model appears to provide a reasonable explanation for why adding oil droplets can shift the SAOS curves of the lab-made aerated taffy closer to those of commercial taffy, as we have observed in Fig. 10. A new species of inclusion with distinct interfacial tension and size distribution is introduced into the sugar matrix, further broadening the relaxation spectrum. The Palierne model also helps rationalize why the SAOS response of the lab-made model taffy appears to be independent of the type of oil used in the taffy recipe [see Fig. 10(c)]. The viscoelastic contribution G_I^* of the inclusions (oil droplets) is likely negligible compared to the dynamic modulus G_M^* of the sugar matrix. Finally, the Palierne model might explain why self-similar relaxation behavior is only evident at low frequencies for the model taffy. It is possible that, unlike commercial taffy, the lab-made model taffy lacks enough small droplets to contribute to the self-similar relaxation behavior observed at higher frequencies. This speculation is consistent with the observation that the lognormal mean inclusion size of the commercial taffy ($\langle d\rangle = 26.7\ \mu$m) is smaller than that of the model taffy ($\langle d\rangle = 35.5\ \mu$m).

Granted that the matrix is a Maxwell fluid like the sugar syrup, that the inclusion is air such that its viscoelastic contribution G_I^* can be neglected, that the size distribution ϕ_i of the air bubbles is lognormally distributed as shown in Fig. 11(b) with $\langle d\rangle = 35.5\ \mu$m, and that

the interfacial tension between sugar syrup and air is the same as that between water and air ($\sigma \approx 70$ mN/m),[62] we find that the Palierne model provides a reasonably accurate prediction for the dynamic moduli of the aerated model taffy ($\phi = c_a = 3$ vol. %) with neither oil nor lecithin added (cf. Fig. 12). Nonetheless, since this inference hinges on several critical assumptions, such an agreement can, at best, be semi-quantitative. Based on this preliminary result, further work will be needed to explore how the Palierne model and other extensions[60,61] can be applied in a quantitative way to more complicated systems, such as to taffy containing both dispersed air and oil phases.

IV. CONCLUSION AND OUTLOOK

In summary, our research delved into the rheology of saltwater taffy, uncovering several key insights into this confection. A key finding is that taffy is thermorheologically simple in the temperature range relevant to taffy processing, i.e., it obeys the time–temperature superposition principle. Application of this principle enabled us to construct master curves representing the linear viscoelastic response of various flavors of commercial taffy across a broad range of timescales at a chosen reference temperature. The dynamic moduli crossover as a sufficiently high frequency is exceeded, at which point the taffy transitions from a dissipative, viscoelastic liquid-like state to a more elastic, solid-like state. We showed that the fractional Maxwell gel (FMG) model can accurately describe the rheology of saltwater taffy in terms of just three parameters: a plateau modulus, a characteristic relaxation time, and a power-law exponent. All master curves for the different taffy flavors considered can be described by the FMG model, and the same power-law exponent applies to each flavor. Scaling the master curves with the individual best-fit values of the plateau modulus and characteristic relaxation time leads to a collapse onto
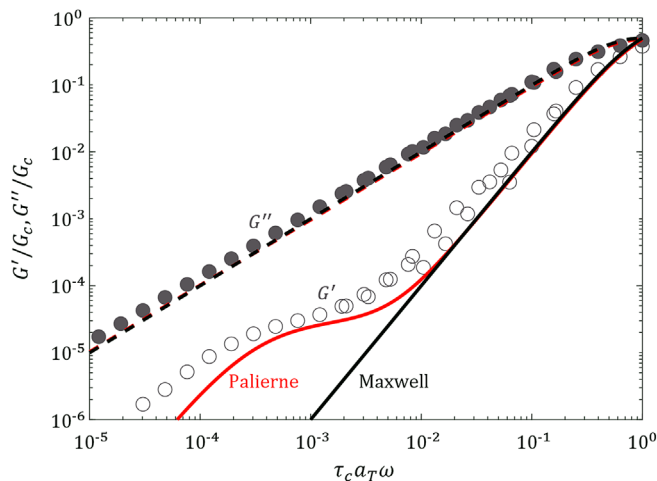
FIG. 12. (a) The scaled dynamic moduli G'/G_c and G''/G_c as functions of the dimensionless reduced frequency $\tau_c \omega_r = \tau_c a_T \omega$ for the aerated model taffy ($c_a = 3$ vol. %) with neither oil nor lecithin added. The black solid and broken lines represent the response of the classical Maxwell model [(4) and (5)]. The red solid and broken lines represent the prediction of the Palierne model (14). The air bubbles are assumed to have the same size distribution as shown in Fig. 11(b) with $\langle d \rangle = 35.5$ μm. The interfacial tension between the sugar syrup and the air is assumed to be $\sigma = 70$ mN/m.

a universal supermaster curve, indicating the presence of a more general time–temperature–taffy superposition (TTTS).

We also probed the rheology of lab-made model syrups with varying water content, finding that they display plateau moduli and relaxation times similar to those of commercial taffy. This observation led us to infer that the linear rheology of taffy at timescales comparable to the relaxation time is governed primarily by their sugar content. We created a second supermaster curve for syrups incorporating different water contents. Guided by the two supermaster curves, we showed that aeration and emulsification progressively shift the rheology of lab-made model taffy away from the purely Maxwell-like response of the sugar syrup matrix and closer to the broad critical gel-like response of commercial taffy. Having found that the rheological behavior of taffy is not affected by the type of oil used in the recipe, we were led to conjecture that the interfacial properties between the inclusions and the sugar matrix underpin the self-similar relaxation behavior of taffy.

Our study focused primarily on the linear viscoelastic response of a specific confection, namely, saltwater taffy, leaving considerable room for future exploration using techniques such as large amplitude oscillatory shear[63] and extensional rheometry.[64] It is unclear whether TTTS also applies to other confections and if so, whether it also applies under large strains. Despite this, the findings of our study on the rheology of taffies and sugar syrups have broader implications for traditional confectionery arts, such as the casting, pulling, and blowing of sugar.[65] We believe that understanding the rheological properties of sugar-based confections might allow artisans to manipulate the material better, leading to novel techniques for creating designs with high artistic and cultural value, as well as enhanced control of their texture and mouthfeel. By uncovering the underlying principles that govern the rheology of these confections, scientists and engineers can contribute to preserving and advancing these culturally significant art forms. Moreover, studying the physical principles associated with manipulating different foods might, in turn, stimulate discoveries of scientific, engineering, and educational importance.[66,67] This approach has already shown value in studying the twisting of Oreo cookies,[68] the tossing of fried rice,[69] the baking of pizza,[70] the fermentation of kimchi,[71] the cooking of pasta,[72] the flipping of burgers,[73] the brewing of coffee,[74] and the pouring of champagne and beer,[75,76] to name a few. We anticipate similar learning outcomes will be obtained by studying the formulation and manipulation of sugar-based confections. Finally, we hope the knowledge gained from this study will foster a renewed appreciation for the history, cultural heritage, and craftsmanship involved in creating these exquisite delicacies, even as automation becomes increasingly dominant in the art and culinary realms.

15 January 2024 08:19:58

AUTHOR DECLARATIONS
Conflict of Interest

The authors have no conflicts to disclose.

Author Contributions

San To Chan: Investigation (lead); Methodology (lead); Writing – original draft (lead). **Simon James Haward:** Investigation (equal); Supervision (equal); Writing – review & editing (equal). **Eliot Fried:** Investigation (equal); Supervision (equal); Writing – review & editing (equal). **Gareth H. McKinley:** Conceptualization (lead); Investigation (equal); Supervision (equal); Writing – review & editing (equal).

DATA AVAILABILITY

The data that support the findings of this study are available from the corresponding author upon reasonable request.

REFERENCES

[1] R. Hartel and A. K. Hartel, *Food Bites: The Science of the Foods We Eat* (Springer, 2008), pp. 175–176.

[2] J. L. Bayline, H. M. Tucci, D. W. Miller, K. D. Roderick, and P. A. Brletic, "Chemistry of candy: A sweet approach to teaching nonscience majors," J. Chem. Educ. **95**, 1307–1315 (2018).

[3] D. Breynard, Saltwater taffy at sweet copper, 2013.

[4] Food Network, Taffy pulling at salty road, 2017.

[5] O. E. Rössler, "The chaotic hierarchy," Z. Naturforsch. A **38**, 788–801 (1983).

[6] M. D. Finn and J. L. Thiffeault, "Topological optimization of rod-stirring devices," SIAM Rev. **53**, 723–743 (2011).

[7] J. L. Thiffeault, "The mathematics of taffy pullers," Math. Intell. **40**, 26–35 (2018).

[8] Chef'n Corporation, Chef'n taffy puller, 2021.

[9] M. van Gurp and J. Palmen, "Time-temperature superposition for polymeric blends," Rheol. Bull. **67**, 5–8 (1998).

[10] L. Berthier and G. Biroli, "Theoretical perspective on the glass transition and amorphous materials," Rev. Mod. Phys. **83**, 587 (2011).

[11] J. Song, N. Holten-Andersen, and G. H. McKinley, "Non-Maxwellian viscoelastic stress relaxations in soft matter," arXiv:2211.06438 (2022).

[12] E. LaBau, Saltwater taffy, 2023.

[13] S. Varchanis, S. J. Haward, C. C. Hopkins, A. Syrakos, A. Q. Shen, Y. Dimakopoulos, and J. Tsamopoulos, "Transition between solid and liquid state of yield-stress fluids under purely extensional deformations," Proc. Natl. Acad. Sci. U.S.A. **117**, 12611–12617 (2020).

[14] F. Ravera, K. Dziza, E. Santini, L. Cristofolini, and L. Liggieri, "Emulsification and emulsion stability: The role of the interfacial properties," Adv. Colloid Interface Sci. **288**, 102344 (2021).

[15] L. Schoeman, P. Williams, A. Du Plessis, and M. Manley, "X-ray micro-computed tomography (μCT) for non-destructive characterisation of food microstructure," Trends Food Sci. Technol. **47**, 10–24 (2016).

[16] A. Du Plessis, C. Broeckhoven, A. Guelpa, and S. G. Le Roux, "Laboratory x-ray micro-computed tomography: A user guideline for biological samples," Gigascience **6**, 1–11 (2017).

[17] F. Snijkers and D. Vlassopoulos, "Cone-partitioned-plate geometry for the ARES rheometer with temperature control," J. Rheol. **55**, 1167–1186 (2011).

[18] T. G. Mezger, *The Rheology Handbook* (Vincentz Network, Hannover, Germany, 2020).

[19] W. N. Findley and F. A. Davis, *Creep and Relaxation of Nonlinear Viscoelastic Materials* (Courier Corporation, 2013).

[20] A. Jaishankar and G. H. McKinley, "Power-law rheology in the bulk and at the interface: Quasi-properties and fractional constitutive equations," Proc. Math. Phys. Eng. Sci. **469**, 20120284 (2013).

[21] G. W. S. Blair, B. C. Veinoglou, and J. E. Caffyn, "Limitations of the Newtonian time scale in relation to non-equilibrium rheological states and a theory of quasi-properties," Proc. R. Soc. London, Ser. A **189**, 69–87 (1947).

[22] A. Bonfanti, J. L. Kaplan, G. Charras, and A. Kabla, "Fractional viscoelastic models for power-law materials," Soft Matter **16**, 6002–6020 (2020).

[23] J. D. J. Rathinaraj, G. H. McKinley, and B. Keshavarz, "Incorporating rheological nonlinearity into fractional calculus descriptions of fractal matter and multi-scale complex fluids," Fractal Fract. **5**, 174 (2021).

[24] B. Keshavarz, D. G. Rodrigues, J. B. Champenois, M. G. Frith, J. Ilavsky, M. Geri, T. Divoux, G. H. McKinley, and A. Poulesquen, "Time–connectivity superposition and the gel/glass duality of weak colloidal gels," Proc. Natl. Acad. Sci. U.S.A. **118**, e2022339118 (2021).

[25] M. Bantawa, B. Keshavarz, M. Geri, M. Bouzid, T. Divoux, G. H. McKinley, and E. Del Gado, "The hidden hierarchical nature of soft particulate gels," Nat. Phys. (published online 2023).

[26] H. H. Winter and F. Chambon, "Analysis of linear viscoelasticity of a crosslinking polymer at the gel point," J. Rheol. **30**, 367–382 (1986).

[27] T. J. Faber, A. Jaishankar, and G. H. McKinley, "Describing the firmness, springiness and rubberiness of food gels using fractional calculus. Part I: Theoretical framework," Food Hydrocoll. **62**, 311–324 (2017).

[28] T. J. Faber, A. Jaishankar, and G. H. McKinley, "Describing the firmness, springiness and rubberiness of food gels using fractional calculus. Part II: Measurements on semi-hard cheese," Food Hydrocoll. **62**, 325–339 (2017).

[29] T. S. K. Ng, G. H. McKinley, and M. Padmanabhan, "Linear to non-linear rheology of wheat flour dough," Appl. Rheol. **16**, 265–274 (2006).

[30] L. Martinetti, A. M. Mannion, W. E. Voje, Jr., R. Xie, R. H. Ewoldt, L. D. Morgret, F. S. Bates, and C. W. Macosko, "A critical gel fluid with high extensibility: The rheology of chewing gum," J. Rheol. **58**, 821–838 (2014).

[31] J. Ahmed, "Time-temperature superposition principles: Applicability in food and biopolymer rheology," in *Advances in Food Rheology and Its Applications* (Elsevier, 2023), pp. 221–260.

[32] K. J. Laidler, "The development of the Arrhenius equation," J. Chem. Educ. **61**, 494 (1984).

[33] S. R. Logan, "The origin and status of the Arrhenius equation," J. Chem. Educ. **59**, 279 (1982).

[34] M. L. Williams, R. F. Landel, and J. D. Ferry, "The temperature dependence of relaxation mechanisms in amorphous polymers and other glass-forming liquids," J. Am. Chem. Soc. **77**, 3701–3707 (1955).

[35] P. Gabarra and R. W. Hartel, "Corn syrup solids and their saccharide fractions affect crystallization of amorphous sucrose," J. Food Sci. **63**, 523–528 (1998).

[36] D. A. Levenson and R. W. Hartel, "Nucleation of amorphous sucrose–corn syrup mixtures," J. Food Eng. **69**, 9–15 (2005).

[37] A. G. Dodson and T. Pepper, "Confectionery technology and the pros and cons of using non-sucrose sweeteners," Food Chem. **16**, 271–280 (1985).

[38] R. W. Hartel and C. M. Nowakowski, "Non-equilibrium states in confectionery," in *Non-Equilibrium States and Glass Transitions in Foods* (Elsevier, 2017), pp. 283–301.

[39] R. G. Larson, Y. Liu, and H. Li, "Linear viscoelasticity and time-temperature-salt and other superpositions in polyelectrolyte coacervates," J. Rheol **65**, 77 (2021).

[40] C. E. Sing and S. L. Perry, "Recent progress in the science of complex coacervation," Soft Matter **16**, 2885–2914 (2020).

[41] S. M. Lalwani, C. I. Eneh, and J. L. Lutkenhaus, "Emerging trends in the dynamics of polyelectrolyte complexes," Phys. Chem. Chem. Phys. **22**, 24157–24177 (2020).

[42] P. Fischer and H. Rehage, "Rheological master curves of viscoelastic surfactant solutions by varying the solvent viscosity and temperature," Langmuir **13**, 7012–7020 (1997).

[43] G. E. Hibberd, "Dynamic viscoelastic behaviour of wheat flour doughs: Part II: Effects of water content in the linear region," Rheol. Acta **9**, 497–500 (1970).

[44] Y. I. Matveev, V. Y. Grinberg, and V. B. Tolstoguzov, "The plasticizing effect of water on proteins, polysaccharides and their mixtures. Glassy state of biopolymers, food and seeds," Food Hydrocoll. **14**, 425–437 (2000).

[45] P. C. Suarez-Martinez, P. Batys, M. Sammalkorpi, and J. L. Lutkenhaus, "Time–temperature and time–water superposition principles applied to poly (allylamine)/poly (acrylic acid) complexes," Macromolecules **52**, 3066–3074 (2019).

[46] G. M. Campbell, "Aerated foods," in *Encyclopedia of Food and Health* (Elsevier Inc., 2016), pp. 51–60.

15 January 2024 08:19:58

[47]G. M. Campbell and E. Mougeot, "Creation and characterisation of aerated food products," Trends Food Sci. Technol. **10**, 283–296 (1999).

[48]M. M. Caruso, D. A. Davis, Q. Shen, S. A. Odom, N. R. Sottos, S. R. White, and J. S. Moore, "Mechanically-induced chemical changes in polymeric materials," Chem. Rev. **109**, 5755–5798 (2009).

[49]F. Awaja, S. Zhang, M. Tripathi, A. Nikiforov, and N. Pugno, "Cracks, micro-cracks and fracture in polymer structures: Formation, detection, autonomic repair," Prog. Mater. Sci. **83**, 536–573 (2016).

[50]M. Razavi, S. Cheng, D. Huang, S. Zhang, and S. Q. Wang, "Crazing and yielding in glassy polymers of high molecular weight," Polymer **197**, 122445 (2020).

[51]U.S. Department of Agriculture, Butter, stick, salted, 2020.

[52]U.S. Department of Agriculture, Oil, coconut, 2019.

[53]U.S. Department of Agriculture, Oil, canola, 2019.

[54]R. W. Hartel, J. H. von Elbe, and R. Hofberger, "Caramel, fudge and toffee," in Confectionery Science and Technology (Springer International Publishing, Cham, 2018), pp. 273–299.

[55]C. Schmidt, R. Bornmann, S. Schuldt, Y. Schneider, and H. Rohm, "Thermo-mechanical properties of soft candy: Application of time-temperature superposition to mimic response at high deformation rates," Food Biophys. **13**, 11–17 (2018).

[56]A. N. Kolmogorov, "On the logarithmically normal law of distribution of the size of particles under pulverization," Dokl. Akad. Nauk SSSR **31**, 99–101 (1941).

[57]J. F. Palierne, "Linear rheology of viscoelastic emulsions with interfacial tension," Rheol. Acta **29**, 204–214 (1990).

[58]D. Graebling, R. Muller, and J. F. Palierne, "Linear viscoelastic behavior of some incompatible polymer blends in the melt. Interpretation of data with a model of emulsion of viscoelastic liquids," Macromolecules **26**, 320–329 (1993).

[59]C. Friedrich, W. Gleinser, E. Korat, D. Maier, and J. Weese, "Comparison of sphere-size distributions obtained from rheology and transmission electron microscopy in PMMA/PS blends," J. Rheol. **39**, 1411–1425 (1995).

[60]C. Lacroix, M. Aressy, and P. J. Carreau, "Linear viscoelastic behavior of molten polymer blends: A comparative study of the Palierne and Lee and Park models," Rheol. Acta **36**, 416–428 (1997).

[61]U. Jacobs, M. Fahrländer, J. Winterhalter, and C. Friedrich, "Analysis of Palierne's emulsion model in the case of viscoelastic interfacial properties," J. Rheol. **43**, 1495–1509 (1999).

[62]N. B. Vargaftik, B. N. Volkov, and L. D. Voljak, "International tables of the surface tension of water," J. Phys. Chem. Ref. Data **12**, 817–820 (1983).

[63]K. Hyun, M. Wilhelm, C. O. Klein, K. S. Cho, J. G. Nam, K. H. Ahn, S. J. Lee, R. H. Ewoldt, and G. H. McKinley, "A review of nonlinear oscillatory shear tests: Analysis and application of large amplitude oscillatory shear (LAOS)," Prog. Polym. Sci. **36**, 1697–1753 (2011).

[64]G. H. McKinley and T. Sridhar, "Filament-stretching rheometry of complex fluids," Annu. Rev. Fluid Mech. **34**, 375–415 (2002).

[65]E. Notter, The Art of the Confectioner: Sugarwork and Pastillage (John Wiley & Sons, 2012).

[66]G. G. Fuller, M. Lisicki, A. J. T. M. Mathijssen, E. J. L. Mossige, R. Pasquino, V. N. Prakash, and L. Ramos, "Kitchen flows: Making science more accessible, affordable, and curiosity driven," Phys. Fluids **34**, 110401 (2022).

[67]A. J. T. M. Mathijssen, M. Lisicki, V. N. Prakash, and E. J. L. Mossige, "Culinary fluid mechanics and other currents in food science," Rev. Mod. Phys **95**, 025004 (2023).

[68]C. E. Owens, M. R. Fan, A. J. Hart, and G. H. McKinley, "On Oreology, the fracture and flow of "milk's favorite cookie$^\circledR$," Phys. Fluids **34**, 043107 (2022).

[69]H. Ko and D. L. Hu, "The physics of tossing fried rice," J. R. Soc. Interface **17**, 20190622 (2020).

[70]P. R. Avallone, P. Iaccarino, N. Grizzuti, R. Pasquino, and E. Di Maio, "Rheology-driven design of pizza gas foaming," Phys. Fluids **34**, 033109 (2022).

[71]S. Kim and D. L. Hu, "Onggi's permeability to carbon dioxide accelerates kimchi fermentation," J. R. Soc. Interface **20**, 20230034 (2023).

[72]J. Hwang, J. Ha, R. Siu, Y. S. Kim, and S. Tawfick, "Swelling, softening, and elastocapillary adhesion of cooked pasta," Phys. Fluids **34**, 042105 (2022).

[73]J. L. Thiffeault, "The mathematics of burger flipping," Physica D **439**, 133410 (2022).

[74]W. T. Lee, A. Smith, and A. Arshad, "Uneven extraction in coffee brewing," Phys. Fluids **35**, 054110 (2023).

[75]O. Atasi, M. Ravisankar, D. Legendre, and R. Zenit, "Presence of surfactants controls the stability of bubble chains in carbonated drinks," Phys. Rev. Fluids **8**, 053601 (2023).

[76]W. Lyu, T. Bauer, A. Jahn, B. Gatternig, A. Delgado, and T. E. Schellin, "Experimental and numerical investigation of beer foam," Phys. Fluids **35**, 023318 (2023).

15 January 2024 08:19:58